Published in final form as:

Loveday, S. M., Creamer, L., Singh, H., & Rao, M. A. (2007). Phase and Rheological Behavior of High-Concentration Colloidal Hard-Sphere and Protein Dispersions. *Journal of Food Science, 72*(7), R101-R107.

doi: 10.1111/j.1750-3841.2007.00452.x

Phase and Rheological Behavior of High-Concentration Colloidal Hard-Sphere and Protein Dispersions

S. M. Loveday, L. K. Creamer, H. Singh, and M. A. Rao

The Riddet Centre, Massey University, Private Bag 11222

Palmerston North, New Zealand

Corresponding author Rao's permanent address: Cornell University, Geneva, NY 14456-0462, USA; email: andy_r_14456@hotmail.com.

Key words: colloidal dispersion, protein, viscosity, glass transition, hard sphere

Abstract

Colloidal hard-sphere particles of narrow-size distribution exhibit crystalline and glassy states beginning at the particle volume fractions ϕ=0.494 and ϕ_G=0.58, respectively. Dynamic rheological data on the dispersions was strongly modified to solid-like behavior as ϕ approached ϕ_G. In addition, cooperative motion in structural relaxation has been observed microscopically in the colloidal dispersions near the glassy state. Very high viscosities and glassy states were also found in high-concentration dispersions of sodium caseinate, and the globular proteins: bovine serum albumin and β-lactoglobulin. Viscosity models developed for hard-sphere dispersions provided reasonable predictions of relative viscosities of colloidal protein dispersions. Dispersions of food colloidal particles may be employed in studies, in which volume fraction is the thermodynamic variable, for understanding the relaxation and transport processes related to first-order and colloidal glass transitions.

Nomenclature

a	particle radius, m
A	coefficient in Equation 5, -
c	concentration, kg m^{-3}
G'	elastic or storage modulus, Pa
G''	loss modulus, Pa
k	Boltzmann constant, 1.38 x 10^{-23} Nm K^{-1}.
T	temperature, K
$\dot{\gamma}$	shear rate, s^{-1}
η	viscosity of a dispersion, Pa s
$[\eta]$	constant in the Krieger-Dougherty equation, -
η_0	zero-shear viscosity, Pa s
η_∞,	high or infinite shear viscosity, Pa s
η_r	relative viscosity, -
η_s	viscosity of continuous phase, Pa s
ϕ	volume fraction of dispersed phase, -
ϕ_{max}	maximum volume fraction of dispersed phase, -
σ	shear stress, Pa

1. Introduction

The size of colloidal (Brownian) particles is not defined rigidly, but generally is considered to range from 1 nm to 1 μm (Russel and others 1989). Such particle sizes are found in foods, such as: milk, cloudy fruit juices, mayonnaise (emulsion). Recently, Genovese and others (2007) reviewed the relevant forces and the rheological behavior of colloidal and non-colloidal dispersions. However, they did not review the phase behavior of those dispersions. In colloidal dispersions, Brownian motion promotes collisions between pairs of colloidal particles and interparticle forces determine if two colliding particles aggregate or not. Brownian motion and interparticle forces quickly equilibrate for nanometer- and sub-nanometer-size dispersions, while hydrodynamic forces dominate for particles larger than ~ 10 μm.

Some foods (ex: chocolate, sauces, starch pastes) contain 'microscopic' particles which are > 10 μm and < ~100 μm (Genovese and others 2007). With these larger particles, Brownian motion and interparticle forces are negligible compared to hydrodynamic forces. But, particle shape, size/size distribution, deformability, and liquid polarity may affect the structure/rheology (Tsai and Zammouri 1988). The different forces that are important in colloidal and non-colloidal dispersions, and their role in rheology have also been noted.

Proteins are found in many natural and formulated foods, and in the natural world. Often, they are encountered in concentrated form so that their phase and rheological behaviors are of interest. Recent studies on hard-sphere (HS) colloidal solids dispersions have yielded fresh insights in to their structural and rheological characteristics. In addition, analogous, if not identical, behaviors have been reported in a few highly-concentrated protein dispersions. For example, it was shown that in hen egg white lysozyme (radius, a≈1.7 nm, molecular mass 14.4 kDa) solutions a combination of short-range attraction and long-range repulsion results in the formation of equilibrium clusters (Stradner and others 2004), and very high viscosities and glassy states are encountered in globular protein dispersions (Farrer and Lips 1999; Brownsey and others 2003; Parker and others 2005). However, it should be noted that while HS solids can be prepared to be spherical, nearly monodisperse, and have well-defined interparticle forces, proteins (globular and non-globular) are non-spherical and control of interparticle forces is not easy.

In this review, we examine the rheological and structural aspects deciphered from experimental studies with hard-sphere colloidal dispersions and contrast them against the results on protein dispersions. We also discuss the potential application of the HS results to food colloidal dispersions and their limitations.

2. Structural Characteristics of Hard Sphere Dispersions

A system of hard spherical particles of uniform size (radius a), each with a volume of $\frac{4}{3}\pi a^3$, suspended in a liquid medium represents a convenient model for experimental, theoretical, and computer simulation studies. However, preparation of nearly-monodisperse, spherical, HS solids with well-defined interparticle forces requires considerable effort. A commonly used model colloidal system for experimental, structural, and rheological studies is sterically stabilized poly-(methyl methacrylate) spheres with a grafted layer of poly (12-hydroxy stearic acid) (PMMA-PHSA) dispersed in a good solvent (typically, decalin or decalin-carbon disulfide) (Krieger 1985; Pusey and van Megen 1986; Phan and others 1996). For example, Pusey and

van Megen (1986) conducted studies using PMMA-PHSA particles of 305 ± 10 nm in decalin and carbon disulphide, volume ratio: 2.66:1.

Studies by different research groups using the model colloidal PMMA-PHSA spheres have led to valuable insights in to their phase and rheological behavior: first, a disordered fluid to crystal transition at ϕ=0.494 and co-existence of crystal and liquid domains for $0.494 \leq \phi \leq 0.545$. Further, as the volume fraction of HSs is increased, transition to fully crystalline state, and finally to a colloidal glassy state. (Pusey and van Megen 1986; Phan and others 1996). The expression "colloidal glass" is used to differentiate it from the well- and long- known temperature-driven glassy state. General phenomena related to the latter have been reviewed by Ediger and others (1996) and others, and in foods by Slade and Levine (1992) and Levine and Slade (1997).

The observations of Pusey and van Megen (1986) on the phase behavior of colloidal HS dispersions are summarized in Figure 1 and they are discussed next. As the solids concentration is increased gradually, at a solids concentration, ϕ=0.494, crystals (clusters of particles) appear that coexist with the liquid. The coexistence of colloidal fluid and crystal phases is analogous to that of a simple liquid and solid at a first-order phase transition. Further, in the coexistence region: $0.494 \leq \phi \leq 0.545$, we find a linear dependence with ϕ which, when extrapolated to 0 and 100%, provides the 'freezing' and 'melting' concentrations. The liquid to crystal transition at ϕ=0.494 is referred to as the beginning of freezing. These observations have been verified by others whose investigations were based on computer simulation, theory, and three-dimensional microscopy (e.g., Phan and others 1996; Weeks and others 2004).

As the volume fraction of solids, ϕ, is increased beyond ϕ=0.545, the particles are increasingly caged by others, and at a critical value, ϕ_G, the caging stops all long-range particle motion, and the system is considered to be glassy (Pham and others 2002). Pusey and van Megen (1986) observed that the highly concentrated (ϕ>0.58), viscous, samples exhibited only partial heterogeneous crystallization even when left undisturbed for several months. The concentration of particles was sufficiently high that particle diffusion was hindered to the point where crystals did not form on that time scale and the suspensions remained in the metastable amorphous phase created by the earlier sample tumbling. Thus, it was concluded that for $\phi \approx 0.58$ hard-sphere colloidal dispersions form glasses.

Further, the glassy state is present over a range of solids concentration. The effective volume fraction of the most concentrated glassy sample was close to ϕ=0.637 expected for the random close-packed HS (so called Bernal) glass. The discovery of a glass composed of equal-sized spheres is especially interesting since, although there has been considerable theoretical work and computer simulations on such model glasses earlier, real glasses composed of spherical units were not identified experimentally. Colloidal glasses were also observed in mixtures of spheres of different sizes (Lindsay and Chaikin 1982), but existence of glassy state in spheres of uniform distribution was noted by Pusey and van Megen (1986). In addition, recently, depending on the range and strength of the attractive and repulsive forces acting between the HSs, computer simulations predicted repulsion-driven and attraction-driven glass transitions that are qualitatively different. This result indicates the possibility of glass-to-glass transitions (Pham and others 2002).

3. Temperature-Driven vs. Concentration-Driven Glass Transition.

Liquids at temperatures below their melting points are called supercooled liquids. Further, cooling a supercooled liquid below the glass transition temperature T_g produces a glass. This macroscopic viscosity divergence is related to the divergence of the microscopic structural relaxation time (α-relaxation time). Microscopically, a glass still has liquid-like structure. However, no structural change has been found which would explain the glass transition

The time scale for molecular motion increases dramatically as a supercooled liquid is cooled toward T_g; rotation times at T_g are typically between 10 and 10^4 s for many materials. These times are much longer compared to the picosecond or nanosecond rotation times observed in typical liquids above T_m. Other measures of molecular mobility also show very large changes as the temperature is lowered toward T_g. In molecular liquids near T_g, it may take many minutes or hours for a very small molecule, e.g., less than 10 Å in diameter, to reorient. (Ediger and others 1996).

A basic concept of many glass transition theories (Adam and Gibbs 1965) is that flow in a supercooled fluid involves cooperative motion of molecules. Further, the structural arrest at the glass transition is due to a divergence of the size of cooperating regions. For nonpolymeric liquids, the slowest relaxation process is called the alpha- (α–) process and roughly corresponds to molecular rotation (Ediger and others 1996). The thermodynamic state of the system deviates from that anticipated by extrapolations of higher temperature measurements and in recent terms, “ergodicity has been broken”. In an ergodic system, ensemble and time averages are equivalent. These two averages are not equivalent in a system evolving toward equilibrium. This means is that molecules have become “stuck” relative to their neighbors so that the volume occupied at the higher temperature tends to be retained, and therefore a change is observed in the system’s expansion coefficient. Computer simulations on supercooled liquids, showed that structural relaxation resulted in the formation of string-like clusters whose size increased as the glass transition temperature was approached (Donati and others 1998). However, there has been no direct experimental observation of these three-dimensional (3D) clusters.

In contrast, using a microscope to directly image particles (Weeks and others 2000), cooperative motion in structural relaxation has been observed in colloidal suspensions. Specifically, three-dimensional confocal microscopy was used to follow the motion of several thousand PMMA-PHSA colloidal particles, radius a=1.18 μm and polydispersity of ~5%, to examine directly how their motion occurs before and at the α-relaxation time scale. The faster-moving particles moved cooperatively in supercooled fluids and formed large extended clusters whose size increased dramatically as the glass transition was approached. In addition, at shorter time scales (β-relaxation) the clusters were much smaller, and similar clusters persisted even for glassy samples.

While temperature is the thermodynamic variable that governs traditional glass transition, the solids content, expressed as volume fraction, ϕ, is the thermodynamic variable in colloidal glass transition. Further, based on findings to date, it appears that with monodisperse colloidal particles a colloidal glass transition is invariably preceded by a first-order fluid-to-crystal transition and it is not a deterrent to finding glassy behavior at high solids concentrations. We note that using silica spheres (radius a =0.21 μm) with a high polydispersity ~20%, Mason and Weitz (1995) found that the colloidal dispersions did not exhibit crystallization; however, they did form a colloidal glass.

4. Rheology of Colloidal Hard Sphere Dispersions

A general shear-thinning curve of apparent viscosity vs. shear rate, that is applicable to HS dispersions, is shown in Figure 2. It has a power law region between two plateau viscosities. It was suggested (Phan and others 1996) that the high shear viscosity, η_∞, is from hydrodynamic forces with a structure displaced far from equilibrium and the zero-shear viscosity, η_0, includes contributions from hydrodynamic forces associated with the equilibrium structure as well as from interparticle and Brownian forces for a structure slightly perturbed from equilibrium. Either η_∞ or η_0 can be used, but the latter appears to be attainable more accurately and conveniently than the former in most rheometers.

The shear stress, σ, at which the viscosity is intermediate between η_0 and η_∞ is of the order of:

$$\sigma \approx kT/a^3 \qquad (1)$$

where, a is the particle radius, T the temperature, and k the Boltzmann constant. For a particle the size of BSA, the calculated value of σ is $\approx 8\times10^4$ Pa so that the observed Newtonian behavior at $\sigma << 10^4$ Pa was equivalent to the η_0 of HS dispersions.

4.1. Relationship Between Viscosity-Volume Fraction.

Models for estimating viscosity of concentrated non-food dispersions of solids are based on volume fraction (ϕ) of the suspended solids and the relative viscosity of the dispersion, $\eta_r = (\eta/\eta_s)$, where η is the viscosity of the dispersion and η_s is the viscosity of the continuous phase (Metzner 1985). At very low solids concentration, the relationship due to Einstein can be used:

$$\eta_r = 1 + 2.5\phi \quad (2)$$

At high concentrations of solids, one widely used equation for dispersions of HSs is that of Krieger-Dougherty (1959) that is based on the assumption that equilibrium exists between individual spherical particles and dumbbells that continuously form and dissociate:

$$\eta_r = \left(1 - \frac{\phi}{\phi_{max}}\right)^{-[\eta]\phi_{max}} \qquad (3)$$

where, $[\eta]$ and ϕ_{max} are the intrinsic viscosity and maximum packing fraction of solids, respectively. Theoretically, $[\eta]$ should be 2.5 for rigid spheres and ϕ_{max} should be about 0.62-0.65 for spheres of uniform diameter (Krieger 1985); however, Choi and Krieger (1986) found it necessary to use values of $[\eta]$ of 2.65 - 3.19.

Phan and coworkers (1996) examined hard-sphere viscosity data reported in the literature over $0<\phi<0.6$ and noted that the magnitudes of relative viscosities obtained on PMMA-PHSA were higher than those on silica and polystyrene spheres. For example, at ϕ=0.5, the relative viscosity of PMMA-PHSA solids was 45±3, while that of silica and polystyrene solids was in the range 24-25.4. They suggested that the PMMA-PSHA solids behaved as hard-spheres up to ϕ =0.60. Also, they fitted all published data on PMMA-PSHA spheres for $0.3<\phi<0.5$ with the equation:

$$\eta_r = [1 - (\phi/\phi_{max})]^{-2} \qquad (4)$$

In Equation 4, a value of $\phi_{max} = 0.577$ was suggested by Phan et al. (1996). It should be noted that the value of $\phi_{max} = 0.577$ was from best curve fit of Equation 4 to the data.

To illustrate the range of relative viscosities associated with the various phases of colloidal HSs discussed earlier, Figures 3 and 4 were drawn to show both the phase and viscosity characteristics of the dispersions. The relative viscosities shown are according to the Krieger-Dougherty model (Equation 3) with $[\eta]$ of 2.50 and ϕ_{max}=0.65, and Equation 4 with $\phi_{max} = 0.577$. For the first-order liquid to crystal transition magnitudes of the relative viscosities, according to the Krieger-Dougherty model (Equation 3) are in the range: 10.2 to 19.3, while those according to Phan and coworkers (1996) are: 48.3 to 325, respectively. The relative viscosity at the beginning of the glassy state of a colloidal HS dispersion, according to the Krieger-Dougherty model, should be > 37.4 at ϕ =0.58 (Figure 4). Values of relative viscosity > 37.4 should be expected from data on PMMA-PHSA spheres; for example, the value calculated using Equation 4 at the lower volume fraction, ϕ =0.50, is 56.2. At higher solids concentration, a dispersion could have values of relative viscosity approaching infinity as $\phi \rightarrow \phi_{max}$; experimental values of globular protein dispersions approaching 1.0 x 10^9 have been reported (Parker and coworkers 2005).

For non-spherical particles, the empirical model of Kitano and others (1981) has been found to be applicable for both synthetic and food dispersions (Rao 2007; Genovese and others 2007):

$$\eta_r = [1 - (\phi / A)]^{-2} \qquad (5)$$

where, the constant *A* is analogous to ϕ_{max} in Equation 4. For rigid particles, the value of *A* decreased as aspect ratio of suspended particles increased; for example, when the aspect ratio was 1.0 (smooth sphere) the magnitude of *A* was found to be 0.68, and when the aspect ratio was 6 to 8 (rough crystal) *A* was 0.44 (Metzner 1985).

4.2. Effect of Polydispersity on Viscosity

For polydispersed spherical particles in Newtonian fluids, ϕ_m is higher since small particles may occupy the space between the larger particles. During flow, they act as a lubricant for flow of the larger particles, thereby reducing the overall viscosity (Servais and others 2002); for a given particle concentration (ϕ), the viscosity decreases with increasing polydispersity (particle size distribution width). For a mixture with different particle size distributions of known particle concentration (ϕ_i), one can use Farris' equation (1968) to estimate the relative viscosity of the mixture as the product of the relative viscosity associated with each discrete unimodal size distribution, $\eta_{ri}(\phi_i)$, assuming no interactions between the particles of different class sizes:

$$\eta_r = \prod_{i=1}^{n} \eta_{ri}(\phi_i) \qquad (6)$$

4.3. Small-Amplitude Oscillatory Tests

Small-amplitude oscillatory tests, also called dynamic tests, can be used to study the viscoelastic properties of HS dispersions. For example, the dependence of the storage modulus, *G'*, and the loss modulus, *G''*, on the oscillatory frequency (ω) in the linear viscoelastic region is one set of useful information. If *G''*>*G'*, the material is behaving predominantly as viscous liquid. However, if *G'*>*G''*, the material is behaving predominantly as a solid. Mason and Weitz (1995) reported that as the volume fraction of the colloidal silica

hard spheres (radius a=0.21 μm) approached that of glass transition, G' became larger than G''. Thus, the dynamic rheological data on the dispersions was strongly modified to solid-like behavior as ϕ approached ϕ_G. Further values of G' as a function of ω developed a plateau, while that of G'' developed a minimum.

5. Structural and Rheological Studies on Protein Dispersions.

Ikeda and Nishinari (2001) reported solid-like behavior, i.e., values of $G'>G''$ over a wide frequency range (0.1 to 100 rad s^{-1}), in 1.0 %w/w, pH 6-7, dispersions of β-LG, bovine serum albumin (BSA), and ovalbumin. While this was an interesting result in that solid-like behavior has been first observed in globular protein dispersions, the protein concentration was very low. More importantly, there was no evidence of a strong transition from a liquid-like to solid-like behavior due to increase in concentration.

5.1. BSA

BSA is a heart shaped globular protein molecule that can be approximated as an equilateral triangle with sides of 8 nm and a depth of 3 nm, and it has an equivalent hydrodynamic radius is 3.7 nm in the range of pH 4 and 8 (Ferrer and others 2001, Brownsey and others 2003). Zero-shear rate and oscillatory shear data were obtained by Brownsey and others (2003) on dispersions with concentrations 20% w/w to 50% w/w and the relative viscosities, calculated using solvent viscosity = 1 mPa s, are shown in Figure 5. It is clear from the figure that the viscosities at very high BSA concentrations increased steeply over a small range of concentrations, as ϕ approached ϕ_{max}. They also estimated values of relative viscosity (solid line) assuming A =0.40 in the Kitano model (Equation 5). However, our estimated values of relative viscosity (dotted line) assuming A =0.44 of the aforementioned rough crystal particle (Metzner 1985) in the Kitano model gave a slightly better fit to the data up to a concentration ~45%.

The frequency dependence of G' and G'' of the 42.5, 47.0, and 50.0 %w/w BSA dispersions were determined over the frequency range 0.01 to 10 Hz. At concentrations <50 % w/w, $G''>G'$. However, at the highest concentration of 50 % w/w, G' crossed G'' at 10 Hz indicating increasing solid-like behavior.

Based on the specific volume of BSA 0.9 ml g^{-1}, derived from their osmotic pressure data, they estimated the volume fraction at the highest viscosity point (Figure 5) to be 0.52. The approach of glass transition at a lower volume fraction than for model HSs was attributed to the non-spherical shape of the BSA molecule. By analogy with the behavior of HS colloidal dispersions, it was suggested that the main structural relaxation results from collective motion over a supra-globule length scale. Further, a secondary relaxation that is more localized and cage-rattling would occur at the globule length scale and additional relaxations specific to molecular nature of the globule would occur at the sub-globule length scale.

5.2. β-Lactoglobulin.

Parker and others (2005) studied the osmotic stress (not discussed here) and the rheological behavior of concentrated β-lactoglobulin (β-LG) dispersions at pH=5.1 and Na Cl concentrations: 0 mM, 100 mM, and 1.0 M. By controlling the pH and the ionic strength, the interparticle attraction was controlled. In steady shear, the zero-shear viscosity of the dispersions was observed at shear rates > 50 s^{-1}. In Figure 6, the viscosity data of the

dispersions are shown as a function of concentration, % w/w, and the marked increase in relative viscosity with concentration of the protein dispersions can be seen.

From small amplitude frequency sweep tests, over ω = 0.02 to 30 Hz, $G''>G'$ for the 45% and 54% w/w protein dispersions, reflecting a viscous liquid-like response. For the 54% w/w dispersion, G' crossed G'' at ω =~2 Hz reflecting a transition to solid-like response. This crossover indicated the approach of a transition comparable to the colloidal glass transition.

An attempt was made to compare the values of relative viscosity based on experimental zero-shear viscosity data with those predicted by the Krieger-Dougherty model (Equation 3). It was noted that the β-LG dimer is not spherical, but can be approximated as a prolate ellipsoid with length=6.9 nm and width=3.6 nm. From literature, the value of ϕ_m=~0.71-0.74 for prolate ellipsoid particles. In addition, in the Krieger-Dougherty model, one can use a vlaue $[\eta]$=3.6 for ellipsoid particles. A specific volume of protein of 0.75 ml g^{-1} was used to obtain the mass of water in the hydrodynamic domain of the protein, and from this the volume fraction of protein at known mass fractions was calculated. Values predicted by the Krieger-Dougherty model were calculated using volume fractions based on two values of apparent protein specific volume: 1.47 ml g^{-1} and 1.12 ml g^{-1} (used in osmotic pressure data). These values are shown in Figure 6 as a solid line and a dashed line, respectively. It can be seen that at higher ionic strength and the mass fraction ~30% (ϕ=~0.5), there was some correspondence between predicted and measured relative viscosities. However, with increasing protein mass fraction, the increase in relative viscosity was less than expected for a HS dispersion.

5.3. Caseins

The structures of caseins were not amenable to examination by X-ray crystallography or high-field NMR examination because they could not be crystallized or to have stable time-invariant three dimensional structures at low pH. The two major caseins are α_{s1}-casein (CN) and β-CN (ca. 35% each of the whole casein mixture). These two proteins behave slightly different from one another and very differently from the well known globular proteins such as serum albumin, lysozyme, and the fibrous proteins that make up muscles, skin etc. Both of these latter classes rely on the hydrogen bonds that form between two protein strands or within a coil formed from a single strand. The former gives rise to the so-called β-sheet and the latter as the α-helix. Panouille and others (2005) suggested that casein is approximately a spherical particle with a mean diameter ~160 nm.

In a mixed casein system, such as sodium cseinate, different caseins interact with each other to form associated structures, which exist as a dynamic system of casein monomers, casein complexes and aggregates (Lucey et al., 2000). The average radius of gyration of caseinate aggregates has been shown to be in the range 22-48 nm, depending upon the method of preparation; the aggregates were shown to be not spherical but highly elongated structures (Lucey et al. 2000).

Towler (1974) examined the flow behavior of 7.5%, 10.0%, and 15.0% rennet casein and sodium caseinate dispersions at shear rates > 10 s^{-1}. For shear rates above 150s^{-1}, the shear rate-shear stress data were described by a modified power law model:

$$\dot{\gamma} = a \exp(b \ln \sigma) \qquad (7)$$

where, a and b are constants. From data over the temperature range 25 °C to 60 °C, the activation energy of flow of the apparent viscosity at 100 s^{-1} was found to be between 29.3 and 51.5 kJ $mole^{-1}$. Carr and others (2002) found that the addition of either monovalent (K^+, Na^+, NH_4^+) or divalent (Ca^{2+}, Mg^{2+}, Zn^{2+}) cations had a major effect on the apparent viscosity

of 14% w/w sodium casein ate solutions. With monovalent salts, the apparent viscosity increased exponentially with ionic strength. It was suggested that, this effect is caused by the salt competing with the casein ate for water and so effectively increasing the protein concentration. For divalent salts the apparent viscosity increased with added ionic strength to a maximum and then decreased again. The decrease was attributed to protein aggregation or idealization

Farer and Lips (1999) obtained zero-shear viscosity data on dispersions of sodium caseinate (pH 6.8, 0.1 M Na Cl) over the range of concentrations ~3 to 28 %w/v. The corresponding values of relative viscosity, calculated using solvent viscosity = 1 mPa s, as a function of sodium caseinate concentration are shown in Figure 7. In the figure, it can be readily seen that the relative viscosity increases gradually with concentration up to about 10% and then steeply at concentrations > 10%. Also shown in Figure 7 (solid line) are values of relative viscosity predicted by the Krieger-Dougherty model with $[\eta]$=2.5 and ϕ_{max}=0.65. It is interesting to note that values predicted by the model are lower than the data up to a concentration of about 14 %w/v, but at higher concentrations they increased more steeply with concentration than the data. This trend is qualitatively similar to that seen for dispersions of BSA (Figure 5) and β-LG (Figure 6).

Panouille and others (2005) also obtained zero-shear viscosity data on dispersions of phosphocaseinate (pH 6.0, polyphosphate 2 %w/v); the phosphocaseinate was obtained after the colloidal calcium phosphate has been removed from the casein. The relative viscosities of the phosphocaseinate dispersions were higher than those of sodium caseinate (Farrer and Lips 1999). An empirical model, based on concentration, *c*, (instead of volume fraction), was used to fit the viscosity data of the phosphocaseinate dispersions up to a concentration of ~10 %w/v:

$$\eta_r = \left(1 - \frac{c}{c_c}\right)^{-2} \qquad (8)$$

The dotted line in Figure 7 represents relative viscosity values of the phosphocaseinate dispersions predicted by the empirical model.

Conclusions

High-concentration dispersions of food colloidal particles, such as globular and other proteins, may be used to create products that are colloidal glasses. Such colloidal glasses should exhibit very high values of apparent viscosities and, in addition, their dynamic rheological behavior should show a strong transition to solid-like behavior as ϕ approached ϕ_G. Because of the uncertainties in the determination of protein particle volume fraction, the polydispersity of the particles, and their softness, rheological models developed for hard-sphere dispersions should provide reasonable, but not accurate, predictions of relative viscosities of colloidal protein dispersions. The dispersions may be used to examine the phase behavior using microscopic and other techniques over a wide range of concentrations, including those approaching and within the colloidal glassy state. Further, the data obtained may be used to calculate structural parameters that shed light on the phase transition.

Additional investigations, are needed in to the structure and rheology of globular and other protein systems in different ionic and pH environments. Also of interest are foods containing proteins that are dehydrated. For example, when a material with average protein concentration of 20 to 35% is subjected to dehydration, vitrification would occur when the protein concentration exceeds 60% w/w and it would have a major effect on transport processes. Vitrification may occur over several length scales and very different water contents, and can include both low-molecular weight solutes and proteins. Particle arrest and vitrification precedes the vitrification of low molecular weight solutes (Brownsey and others 2003). Other foods, such as chocolates, with medium to high solids volume fraction and low attractive or repulsive interaction energy may also exhibit a glass transition at rest caused by crowding of the particles (Servais and others 2004).

References

Adam G, Gibbs JH. 1965. On the temperature dependence of cooperative relaxation properties in glass-forming liquids. Journal of Chemical Physics. 43:139-146.

Brownsey GJ, Noel TR, Parker R, Ring, SG. 2003. The glass transition behavior of the globular protein Bovine Serum Albumin. Biophysical Journal 89:3943-3950.

Carr AJ, Munro, PA, Campanella, OH. 2002. Effect of added monovalent or divalent cations on the rheology of sodium caseinate solutions. Int. Dairy Journal 12:487–492

Choi GR, Krieger IM. 1986. Rheological studies on sterically stabilized model dispersions of uniform colloidal spheres II. Steady-shear viscosity. Journal of Colloid and Interface Science 113:101-113.

Donati C, Douglas JF, Kob W, Plimpton SJ, Poole PH, Glotzer SC. 1998. Stringlike cooperative motion in a supercooled liquid. Physical Review Letters 80:2338-2341.

Ediger MD, Angell CA, Nagel SR. 1996. Supercooled liquids and glasses. J. Phys. Chem. 100:13200-13212.

Farrer D, Lips A. 1999. On the self-assembly of sodium caseinate. International Dairy Journal 9:281-286.

Ferrer ML, Duchowicz R, Carrasco B, Torre JG, Acuña AU. 2001. The conformation of serum albumin in solution: A combined phosphorescence depolarization-hydrodynamic modeling study. Biophysical Journal 80:2422–2430.

Genovese DB, Lozano J, Rao MA. 2007. The rheology of colloidal and non-colloidal food dispersions. J Food Science 72:R11-R20.

Ikeda S, Nishinari K. 2001. On solid-like rheological behaviors of globular protein solutions. Food Hydrocolloids 15:401-406.

Kitano T, Kataoka, T, Shirota T. 1981. An empirical equation of the relative viscosity of polymer melts filled with various inorganic fillers. Rheologica Acta 20:207-209.

Krieger IJ. 1985. Rheology of polymer colloids. In *Polymer Colloids*, eds. R. Buscall, T. Corner, J. F. Stageman, pp. 219-246, Elsevier Applied Science, New York.

Krieger IM, Dougherty TJ. 1959. A mechanism for non-Newtonian flow in suspensions of rigid spheres. Transactions Society of Rheology 3:137-152.

Levine H, Slade L. 1992. Glass transition in foods, in *Physical Chemistry of Foods*, H. G. Schwartzberg R. W. Hurtle, p. 83-221, Marcel Decker, New York.

Lindsay HM, Chaikin PM. 1982. Elastic properties of colloidal crystals and glasses. Journal of Chemical Physics 76(7):3774-3781.

Lucey JA, Srinivasan M, Singh H, Munro PA. 2000. Characterisation of commercial and experimental sodium caseinates by multi-angle laser light scattering and size-exclusion chromatography. JAgricultural Food Chem. 48:1610-1616.

Mason TG, Weitz, DA. 1995. Linear viscoelasticity of colloidal hard sphere suspensions near the glass transition. Physical Review Letters 75:2770-2773.

Metzner AB. 1985. Rheology of suspensions in polymeric liquids. J. Rheology 29:739-775.

Panouille M, Benyahia L, Durand D, Nicolai T. 2005. Dynamic mechanical properties of suspensions of micellar casein particles. Journal of Colloid and Interface Science. 287:468-475.

Parker R, Noel TR, Brownsey GJ, Laos K, Ring SG. 2005. The nonequilibrium phase and glass transition behavior of β-Lactoglobulin. Biophysical J 89:1227-1236.

Pham KN, Puertas AM, Bergenholtz J, Egelhaaf SU, Moussaid, A Pusey PN, Schofield AB, Cates ME, Fuchs M, Poon WCK. 2002. Multiple glassy states in a simple model system. Science 296:104-106.

Phan S-E, Russel, WB, Cheng Z, Zhu J, Chaikin PM, Dunsmuir JH, Ottewill RH. 1996. Phase transition, equation of state, and limiting shear viscosities of hard sphere dispersions. Physical Review E 54:6633-6645.

Pusey PN, van Megen W. 1986. Phase behaviour of concentrated suspensions of nearly hard colloidal spheres. Nature 320:340-342.

Rao, MA. 2007. Rheology of Fluid and Semisolid Foods: Principles and Applications, 2nd ed. New York: Springer 480 p.

Russel WB, Saville DA, Schowalter WR. 1989. Colloidal dispersions. Ed. G.K. Batchelor. Cambridge, UK: Cambridge University Press. 525 p.

Servais C, Jones R, Roberts ID. 2002. The influence of particle size distribution on the processing of food. J Food Eng 51:201-8.

Servais C, Ranc H, Roberts ID. 2004. Determination of chocolate viscosity. J. Texture Studies. 34(5-6):467-498

Slade L, Levine H. 1998. Selected aspects of glass transition phenomena in baked goods, in *Phase/State Transitions in Foods*, eds. M. A. Rao R. W. Hartel, p. 87–94, Marcel Dekker, New York.

Stradner A, Sedgwick H, Cardinaux F, Poon WCK, Egelhaaf SU, Schurtenberger P. 2004. Equilibrium cluster formation in concentrated protein solutions and colloids. Nature 432:492-495.

Towler C. 1974. Rheology of casein solutions. NZ J Dairy Sci Tech 9:155-160.

Tsai SC, Zammouri K. 1988. Role of interparticular van der Waals force in rheology of concentrated suspensions. J Rheol 32(7):737-50.

Weeks ER, Crocker JC, Levitt AC, Schofield A, Weitz DA. 2000. Three-dimensional direct imaging of structural relaxation near the colloidal glass transition. Science 287:627-631.

Figure 1. Phase behavior of colloidal hard sphere dispersions, based on Pusey and van Megen (1986).

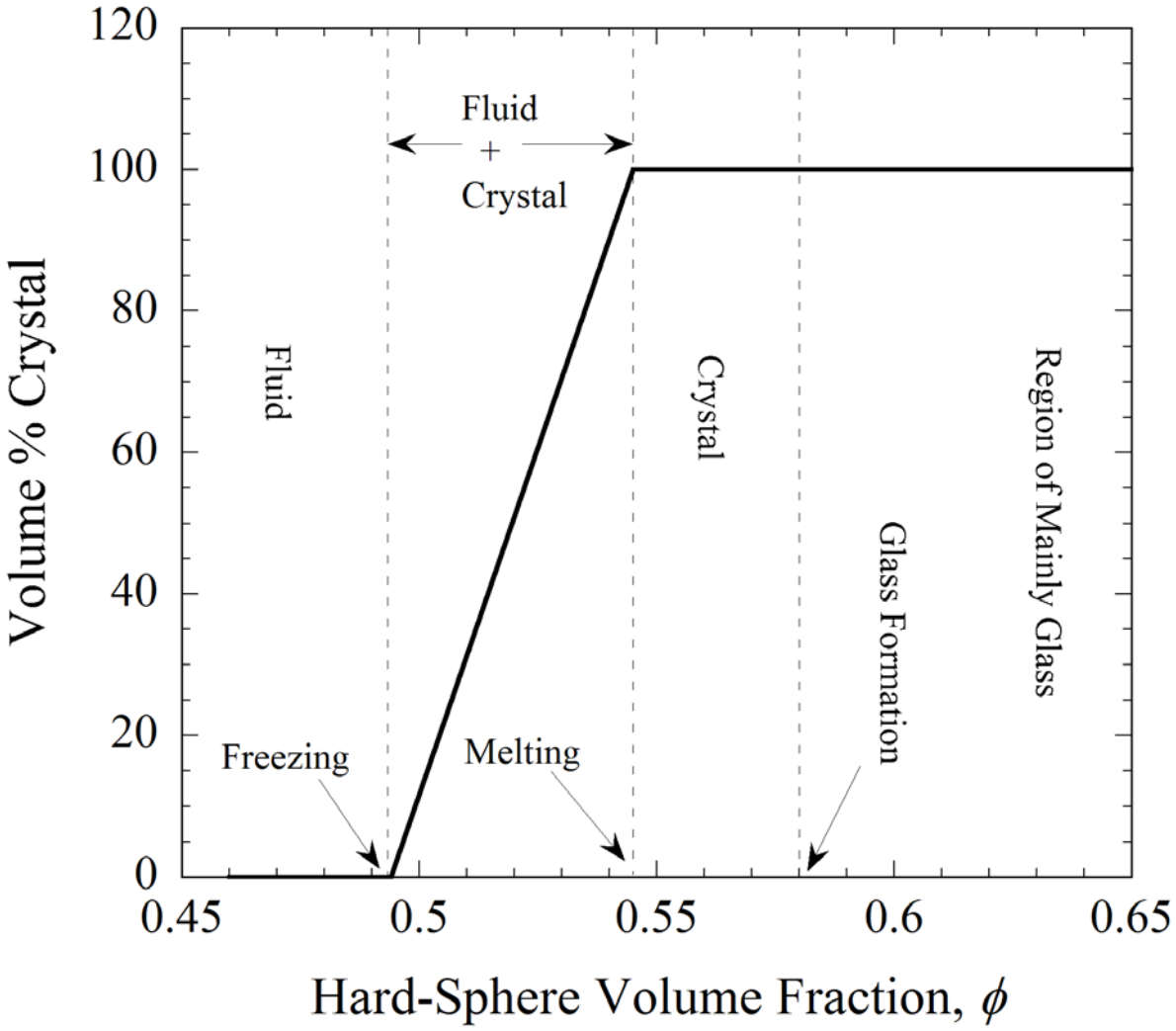

Figure 2. General apparent viscosity vs. shear rate curve of colloidal dispersions with power law region between zero- and infinite-shear viscosities.

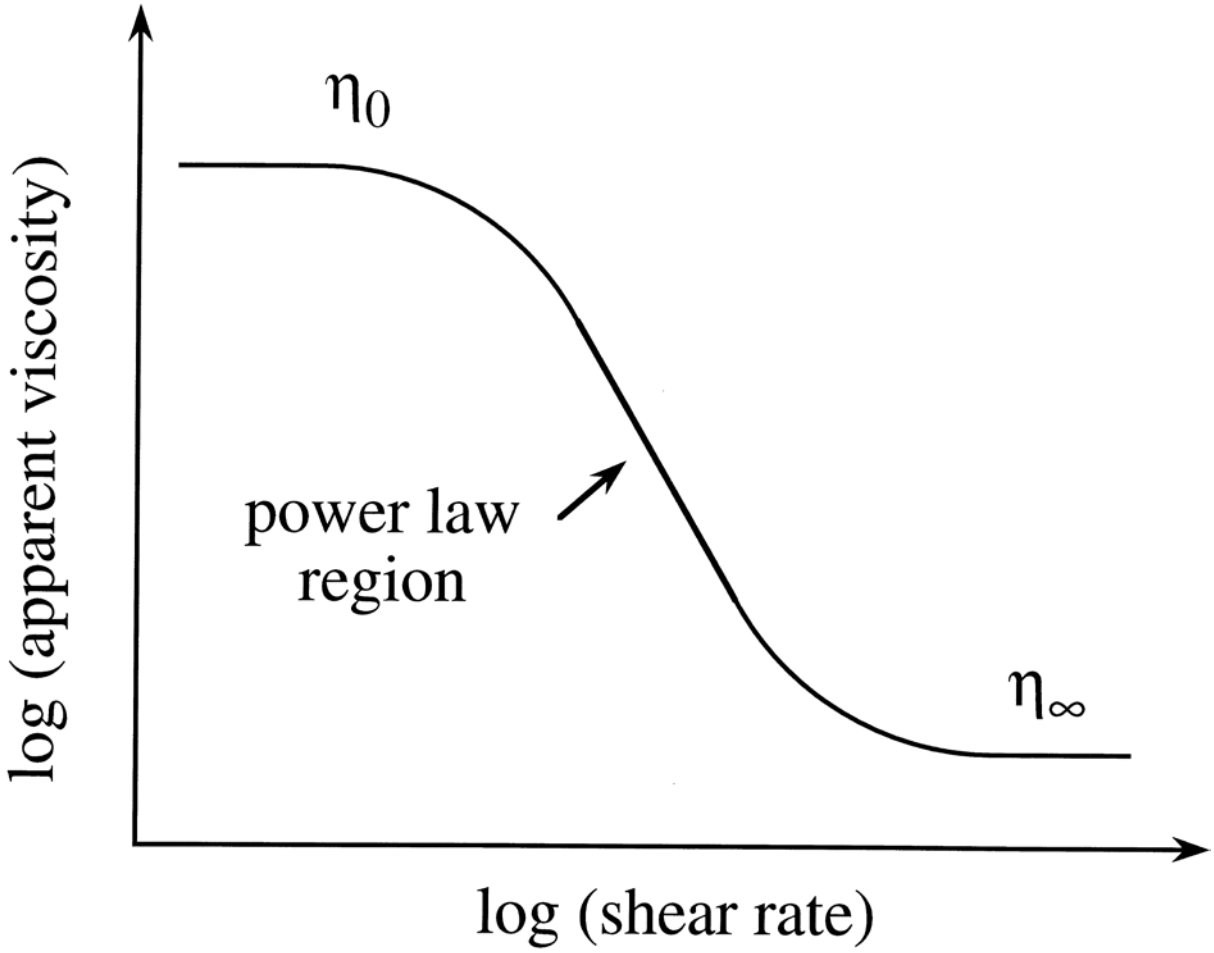

Figure 3. First-order, fluid-to-crystal, phase change, and relative viscosities of hard-sphere colloidal dispersions according to Krieger and Dougherty (1959), and Phan and others (1996).

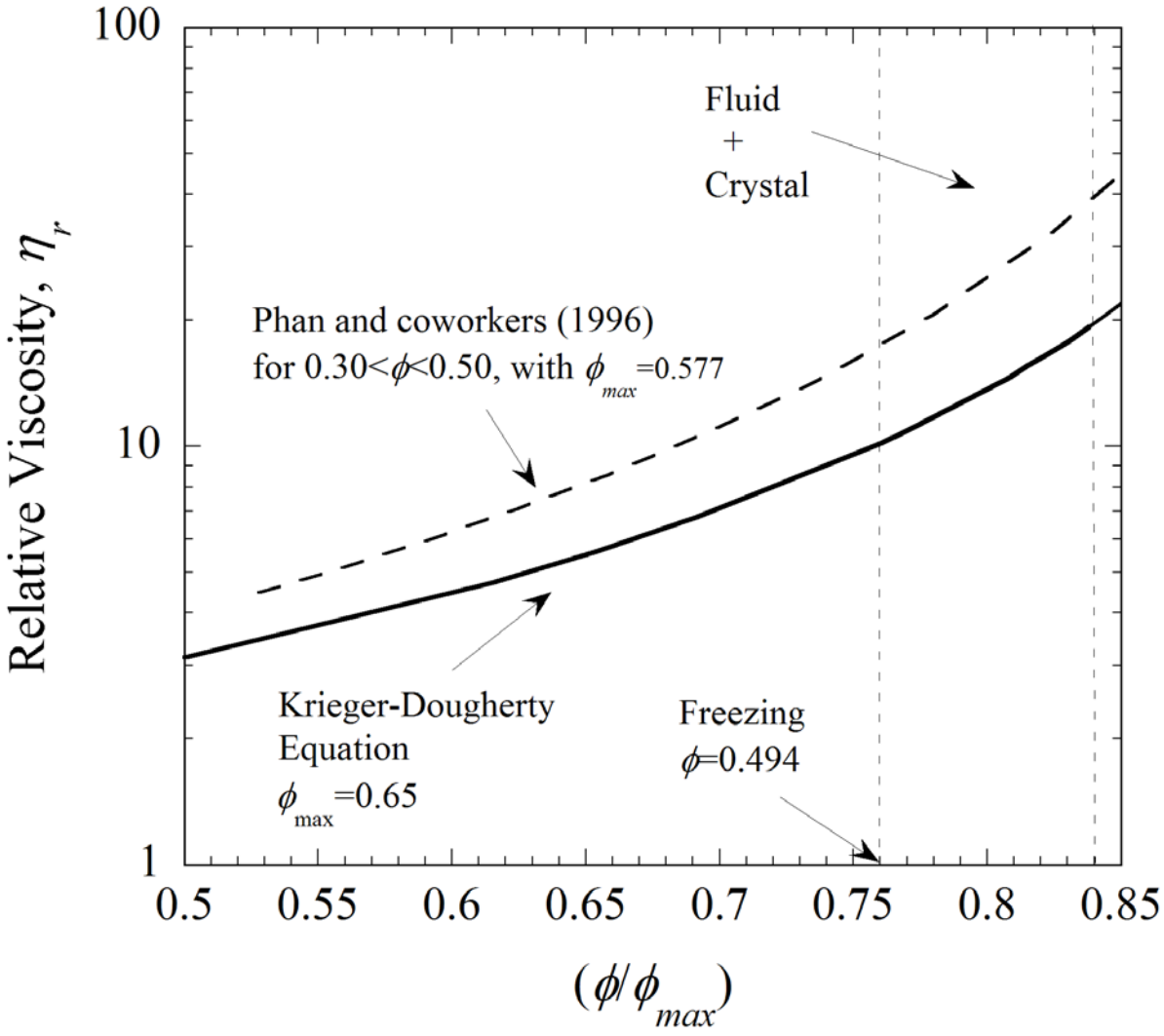

Figure 4. Glass transition superposed on the relative viscosities of hard-sphere colloidal dispersions according to Krieger and Dougherty (1959), and Phan and others (1996).

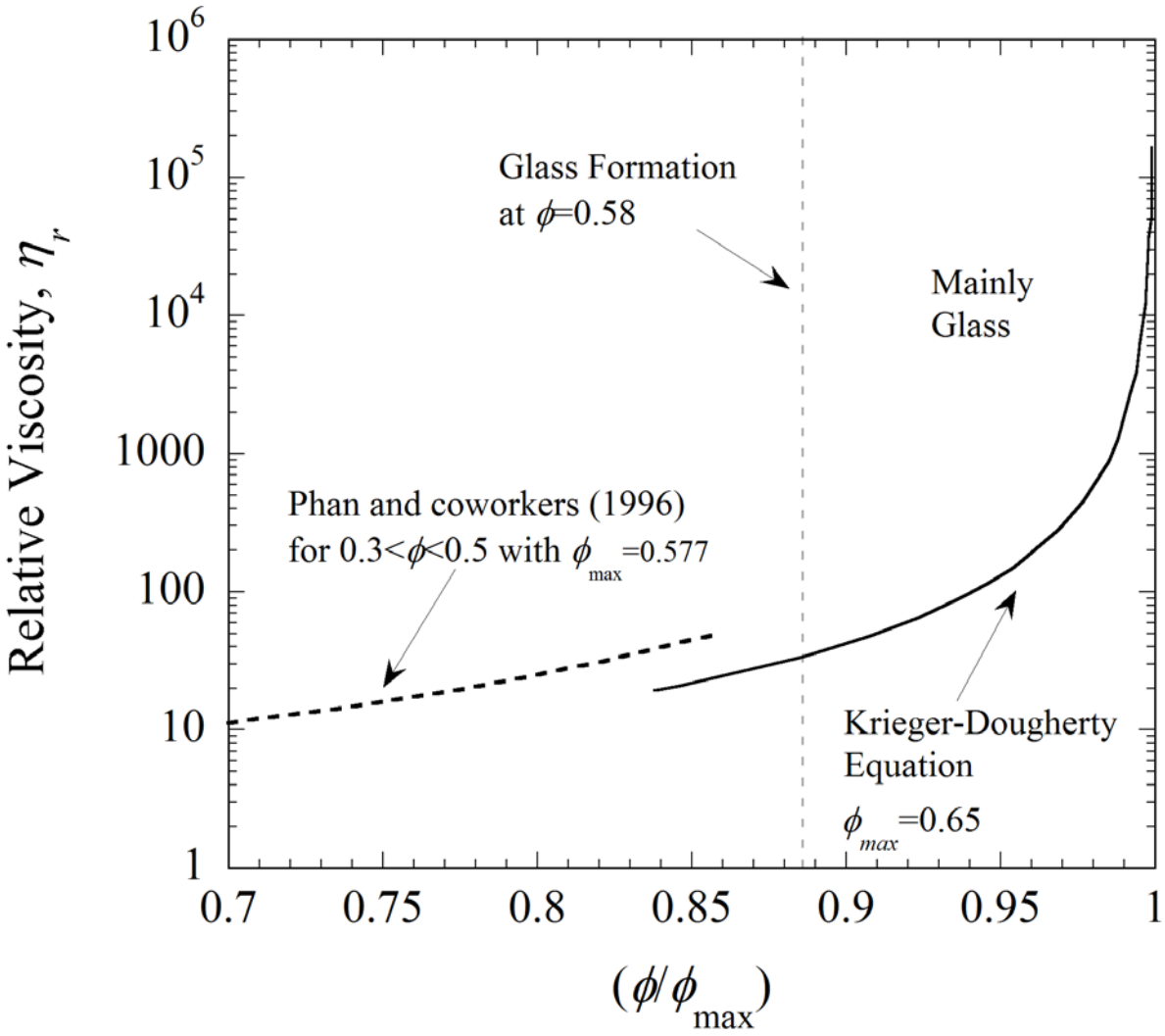

Figure 5. Relative viscosity vs. concentration data on aqueous bovine serum albumin dispersions (Brownsey and others 2003): steady shear data, ●, and oscillatory shear data, ▲. Values estimated using the model of Kitano and coworkers (1981): solid line, A=0.40 and dotted line A=0.44.

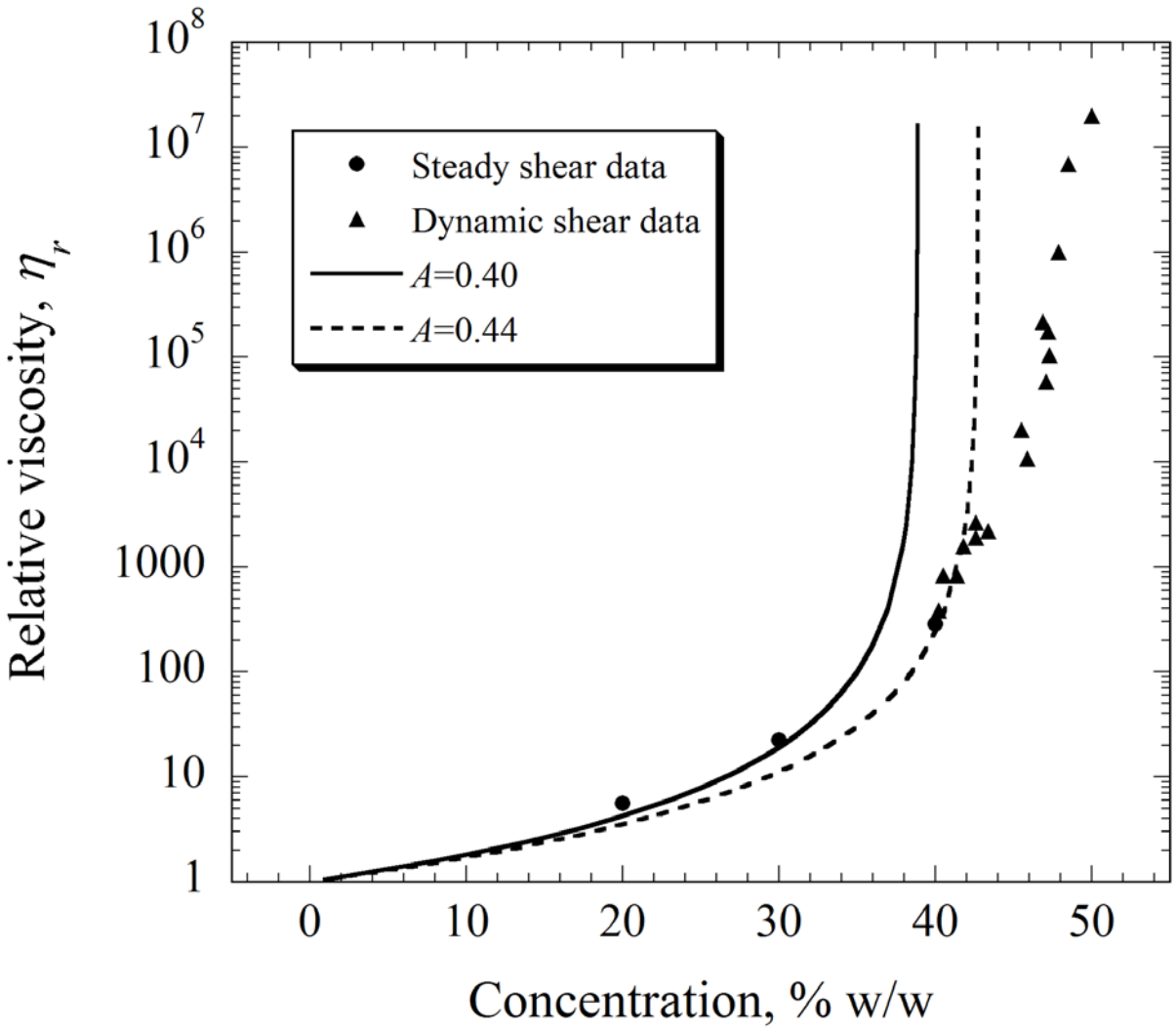

Figure 6. Relative viscosity of β-lactoglobulin dispersions at pH 5.1 and three NaCl concentrations. Also shown are values predicted by the Krieger and Dougherty (1959) model with $[\eta]$=3.6 and ϕ_{max}=0.71 assuming two values of apparent specific volume: 1.47 ml g^{-1} (solid line) and 1.12 ml g^{-1} (dotted line).

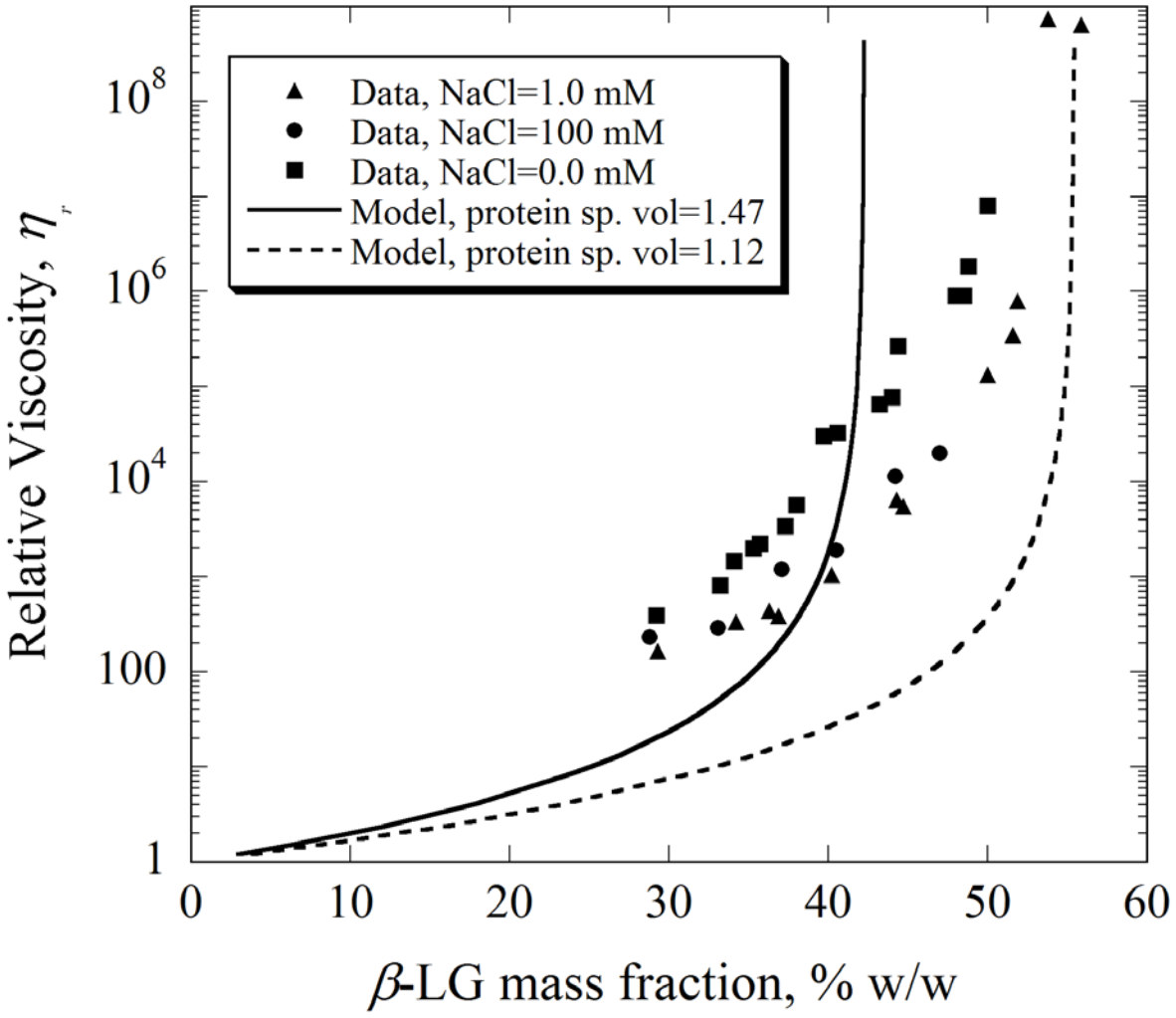

Figure 7. Data of Farrer-Lips (1999) on dispersions of Na caseinate pH=6.8, 0.1 M NaCl. Solid line: values using the Krieger and Dougherty (1959) model for hard spheres with $[\eta]$=2.5 and ϕ_{max}=0.65. Dotted line: values calculated using equation that fit data on dispersions of phosphocaseinate (pH 6.0, polyphosphate 2 %w/v) in water by Panouille and others (2005).